Toward a Reliable Description of the Lattice Vibrations in Organic Molecular Crystals: The Impact of van der Waals Interactions

Towards a reliable description of the lattice vibrations in organic molecular crystals: the impact of van der Waals interactions

Natalia Bedoya-Martínez,*,† Andrea Giunchi,‡ Tommaso Salzillo,‡ Elisabetta Venuti,‡ Raffaele Guido Della Valle,‡ and Egbert Zojer*,†

†*Institute of Solid State Physics, NAWI Graz, Graz University of Technology, Petersgasse 16, 8010 Graz, Austria*

‡*Department of Industrial Chemistry "Toso Montanari", University of Bologna, Viale Risorgimento 4, I-40136 Bologna, Italy*

E-mail: bedoyamartinez@tugraz.at; egbert.zojer@tugraz.at

Abstract

This work assesses the reliability of different van der Waals (vdW) methods to describe lattice vibrations of molecular crystals in the framework of density functional theory (DFT). To accomplish this task, calculated and experimental lattice phonon Raman spectra of a pool of organic molecular crystals are compared. We show that the many-body dispersion (MBD@rsSCS) van der Waals method of Ambrosetti et al., and the pair-wise method of Grimme et al. (D3-BJ) outperform the other tested approaches (i.e. the D2 method of Grimme, the TS method of Tkatchenko and Scheffler, and the non local functional vdW-DF-optPBE of Klimeš et al.). For the worse-performing approaches the results could not even be fixed by the introduction of scaling parameters, as commonly used for high-energy intramolecular vibrations. Interestingly, when using the experimentally determined unit cell parameters, DFT calculations using the

1

PBE functional without corrections for long-range vdW interactions provide spectra of similar accuracy as the MBD@rsSCS and D3-BJ simulations.

1 Introduction

Organic semiconductors, due to their unique features and advantages (earth-abundant raw materials, low-cost deposition, light weight and flexibility), are very attractive for electronic and optoelectronic applications. Light-emitting diodes, field-effect transistors, and photovoltaics devices are examples of the wide range of emerging devices based on organic semiconductors. These materials, thus, are in the focus of many investigations that seek to understand, characterize, and improve their physico-chemical properties.

Among the many interesting properties of organic semiconductors, their vibrational properties are of considerable importance. For instance, they are relevant to understand the mechanisms that govern various transport processes: dynamic disorder originating from intermolecular vibrations is considered a limiting factor for the charge transport across organic semiconductors.[6–9] Vibrations are also crucial for thermal transport in these materials, which typically feature very low thermal conductivities[10] that can be highly anisotropic.[11]

An understanding of the vibrations of organic molecular semiconductors at an atomistic level can drive the development of strategies to design new materials with improved transport properties. This could be done by identifying and suppressing the vibrations responsible for dynamic disorder, or by employing molecular design for controlling those phonons that contribute most to heat transport.

From a computational point of view, the ability to correctly predict vibrational properties in organic molecular semiconductors depends on the accuracy of the model to describe forces within (intramolecular) and between (intermolecular) molecules. Density functional theory (DFT) has proven rather accurate for the description of intramolecular interactions at reasonable computational cost. Still a slight overestimation of vibrational energies can

arise from the lack of anharmonicities in the calculations, the incomplete incorporation of electron correlation and the use of finite basis sets.[12] This overestimation, however, has been shown to be systematic and can be corrected by the use of scaling parameters.[12,13]

In contrast, DFT calculations in the low-wavenumber spectral region (< 150 cm^{-1}) are more challenging. There, intermolecular vibrations dominate and vdW-interactions are expected to become critically important. Unfortunately, (semi)local DFT functionals do not account for the long-range attractive part of vdW-interactions, and appear unsuitable to describe the vibrations of organic molecular crystals in that spectral region. Notably, those vibrations are particularly important, as they determine the charge and heat transport properties of molecular materials.

Multiple approaches to account for the long-range attractive part of vdW-interactions[14] in semi(local) DFT have been proposed in the past years.[15,16] These include non-local functionals,[17,18] modified pseudo-potentials,[19] and a posteriori interatomic (pairwise or beyond) vdW-correction methods.[1,2,4,20–29] The accuracy and reliability of these methodologies to describe binding and cohesive energies, and to predict crystalline structures, have been extensively addressed. Few works, however, report on the reliability of vdW-corrected DFT methods to describe intermolecular vibrations.[30–35] Particularly, the lack of experimental data has precluded a conclusive test.

Here we report a detailed benchmark of four a posteriori vdW-corrected DFT methods to describe intermolecular vibrations. The reliability of the vdW-methods is assessed by comparing calculated and measured lattice Raman spectra in the low wave number region (< 150 cm^{-1}) of in total five polymorphs of three different organic semiconductors. We deem the study of different polymorphs of crystals consisting of identical molecules particularly relevant, as there differences in intermolecular interactions should have a strong impact. While being rather exhaustive in the choice of test systems, including all possible flavors of vdW-corrections would go beyond the scope of the present manuscript. Therefore, we concentrated on a posteriori vdW-correction schemes including the pairwise D2-method of

Grimme,[3] (one of the first widely used van der Waals correction), the more advanced D3-BJ method of Grimme et al.[2] (containing geometry-dependent pairwise parameters), the TS pairwise method of Tkatchenko and Scheffler[4] (considering the local environment of an atom through its Hirshfeld charge), and the many-body dispersion approach (MBD@rsSCS) as proposed by Ambrosetti et al..[1] Albeit not in the focus of the present study, for the sake of comparison, a non-local functional[5,36] was also tested for the polymorphs of one of the systems considered. Additionally, we assessed how well the spectra are reproduced by pure semi-local DFT disregarding van der Waals corrections.

2   Methods

Simulations were performed in the framework of DFT using the VASP package (version 5.4.1).[37–40] The Perdew-Burke-Ernzerhof (PBE) exchange and correlation functional was used in combination with the projector-augmented wave (PAW) approach.[41,42] The specific versions of the PAW potentials employed for each element are reported in Table 1s in the Supporting Information.

To sample the Brillouin zone, the converged Monkhorst-Pack k-point grids listed in Table 2s in the Supporting Information were used. They were chosen such that total energies per atom were converged to at least 0.03 meV. A plane wave cut-off energy of 800 eV was used for all calculations, ensuring a convergence of 0.7 meV/atom compared to a cutoff of 1200 eV. As shown in Figure 1s and Table 3s in the Supporting Information, phonon frequencies are calculated with an accuracy of $\ll 0.7$ cm^{-1} by using this cutoff. The total energy during the self-consistency loop of each DFT step was converged to 10^{-8} eV.

Calculations were performed using both the experimental volume (V_{exp}) and the relaxed volume (V_{calc}) predicted by the corresponding vdW-DFT approach. Atomic relaxations in both cases were performed with a threshold of 10^{-3} eV Å^{-1} for the residual forces using the GADGET tool.[43] Additionally, for volume relaxations zero external pressure has been

4

imposed.

The distance comparison method was used to quantify the differences between the experimental and calculated relaxed cells. Accordingly, all interatomic distances between a reference molecule and a suitable number of neighbors within the same structure were listed. Subsequently, experimental and calculated structures were compared by means of the root-mean-square-deviation (RMSD) between their lists of distances.[44]

Phonon frequencies were obtained either by finite differences, using the PHONOPY simulation package[45] in combination with VASP, or by using density functional perturbation theory (DFPT) [depending on the availability of DFPT for the tested vdW-methods in the VASP package]. The calculations based on finite differences were performed using the default value for the atomic displacement distance defined within PHONOPY (i.e. 0.01 Å). This provides frequencies that are in perfect agreement with those predicted by DFPT (as shown for one system in Figure 2s and Table 4s in the Supporting Information). The precision flag for all VASP calculations was set to "ACCURATE", as very accurate forces were required. For comparison to Raman spectra it was sufficient to calculate phonons at the Γ point.

The resulting phonon properties (eigenfrequencies and eigenvectors) were used to calculate Raman spectra. In practice we first identified those modes that are Raman active for each system, by applying the symmetry operations of the corresponding crystal on the calculated eigenvectors. Subsequently, we calculated the isotropic Raman intensities employing the method of Porezag and Pederson[46] as implemented in the Python program VASP_RAMAN.PY,[47] which uses the VASP code as backend.

The temperature dependence of the Raman intensities was included by using the Bose occupation factor, $1+n(\omega) = [1-\exp(-h\nu_i/k_{\mathrm{B}}T)]^{-1}$, calculated at $T = 300$ K (temperature at which experiments were performed). Here ν_i is the frequency of a mode i, and k_{B} denotes the Boltzmann constant. The Lorentzian functions around the calculated peak positions (with intensities I_i) on the reported Raman spectra were obtained from $I(\nu) = \sum_i I_i \frac{\Gamma}{(\nu-\nu_i)^2+\Gamma^2}$, with $\Gamma = 1.5\,\mathrm{cm}^{-1}$.

Four different vdW-approaches were benchmarked, namely: (i) the pairwise D2 approach of Grimme,[3] that consists in adding pairwise interatomic terms, $C_6 R^{-6} f$, to the total energy. Here the C_6 parameters are tabulated coefficients describing the strength of the interaction, and f is a function to damp the vdW correction upon approaching bonding distances. (ii) The improved pairwise approach of Grimme et al. in combination with the Becke-Johnson damping function (D3-BJ),[2] which in addition to the $C_6 R^{-6} f_6$ terms adds extra contributions, $C_8 R^{-8} f_8$, to the total energy. Here the coefficients and the damping functions are adjusted on the basis of the local geometry (coordination number). (iii) The pairwise TS approach of Tkatchenko and Scheffler,[4] which has the same functional form as the D2 method. In this case, however, the C_6 parameters and damping function depend on the (Hirshfeld) charge of the atoms taking the local environment into account. (iv) The MBD@rsSCS approach of Ambrosetti et al.,[1] that goes beyond pairwise interactions, and accounts for long-range electrostatic screening. Here, the MBD@rsSCS-energy contribution depends on the frequency-dependent polarizability matrix, and the long-range interaction tensor. The latter describes the interaction of the screened polarizabilities embedded in the system in a given geometrical arrangement.[28]

As mentioned above, for the polymorphs of one system we also tested the non-local functional method of Dion et al.[17] as optimized by Klime et al. for PBE (optPBE).[5,36]

The experimental Raman spectra used in this work were previously published,[48–50] and correspond to unpolarized measurements. In the following we will focus on comparing peak positions rather than intensities, as there is a (typically unknown) degree of texturing of the samples. The wavenumbers used to label the experimental peaks were taken from polarized Raman spectra, reported in the original publications.

3 Results and discussion

Among the many different organic molecular crystals reported in literature, this work focuses on crystalline polymorphs of organic molecules for which experimental lattice Raman spectra in the low-wavenumber region are available.[48–50] In total, five systems were considered in the benchmark test, comprising polymorphs of the molecules: (i) dibenzo-tetrathiafulvalene (DB-TTF),[48,49] (ii) 9,10-diphenylanthracene (DPA),[50,51] and (iii) 2,7-diocty loxy[1]benzothieno[3,2-b]benzothiophene (OBTBT).[52,53]

Figure 1 shows the corresponding unit cells, and introduces the notation used throughout the paper. The chosen systems vary in structural details relevant for intermolecular interactions: in the case of DB-TTF, the considered polymorphs have two molecules per unit cell arranged in a herringbone structure, that crystallize either in a monoclinic (α-phase) or triclinic (δ-phase) structure. The main difference between the two polymorphs is the intermolecular distance along the stacking direction, which is shorter in the α-phase of DB-TTF (stacking along $\vec{c}$) than in the δ-phase of DB-TTF (stacking along $\vec{a}$). While DB-TTF comprises a rigid molecule, DPA features torsional degrees of freedom between the phenyl unit and the anthracene core. In this case two polymorphs of the DPA molecule were considered, both crystallizing in a monoclinic structure with four molecules in the unit cell. The α- and γ-phase of DPA differ in the dihedral angle formed by the planes of the antracene and the phenyl, which for the α-phase is $\sim 68^o$ while for the γ-phase it is $\sim 89^o$. Finally, the PS-phase of OBTBT represents a prototypical example of a molecule consisting of a rigid-conjugated backbone with flexible aliphatic side-chains.
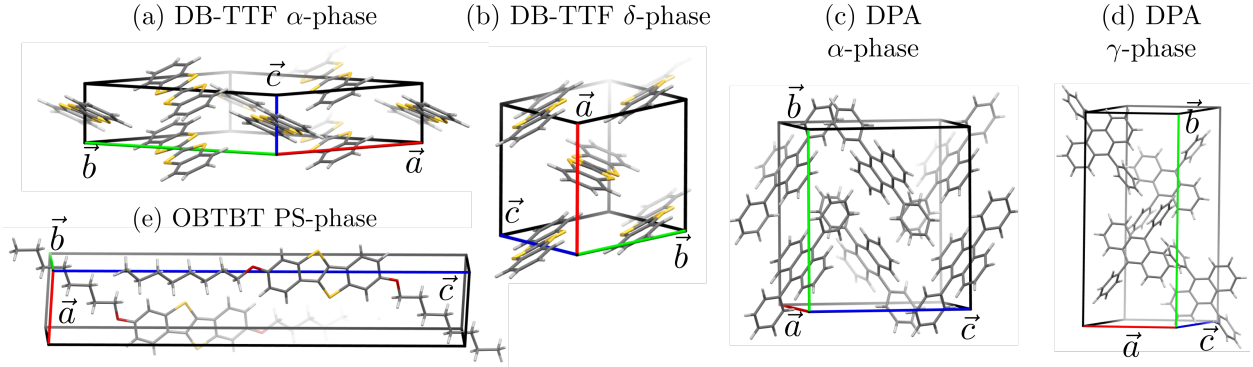
Figure 1: Unit cells of the considered crystals. (a) α and (b) δ polymorphs of the DB-TTF molecule. (c) α and (d) γ polymorphs of the DPA molecule. (e) Parallel-stacked (PS) polymorph of the OBTBT molecule. Gray, white, yellow and red colors denote carbon, hydrogen, sulfur and oxygen atoms.

In the following, we will first assess the performance of the different methods on the basis of experimentally determined unit cells. On the one hand, we will benchmark the simulated Raman spectra against the experimental ones. On the other hand, we will compare the calculated frequencies and displacement patterns obtained with the MBD@rsSCS method (chosen as reference) to those obtained with all other van der Waals correction schemes. Subsequently, we will test how well experimental unit cell geometries are reproduced with the different vdW-methods by relaxing the cell parameters. Finally, we will show for the methodologies performing best and worst in the original assessment, how switching from the experimental to the theoretical cell parameters impacts the Raman spectra.

3.1 Calculated Raman spectra using experimental unit cell parameters

Very recently we showed that the MBD@rsSCS method can predict lattice vibrations for the polymorphs of the OBTBT molecule within an accuracy of $\ll 5$ cm^{-1}, provided that the experimental volumes are known.[32] The same order of accuracy is obtained in all calculations employing the MBD@rsSCS vdW correction for the pool of molecular crystals considered in this work (see purple curves in Figs. 2-4). In most instances, the experimentally observed

8

peaks can be clearly identified within the MBD@rsSCS Raman spectra. This allows associating measured vibrational modes with specific (calculated) displacement patterns (i.e. eigenmodes), which is not possible from the experimental data alone. This assignment is crucial for understanding vibrational dependent properties of materials, such as heat or charge transport. The MBD@rsSCS calculated spectra, in addition, provide insight regarding the actual number of Raman active modes contributing to the experimental spectrum.
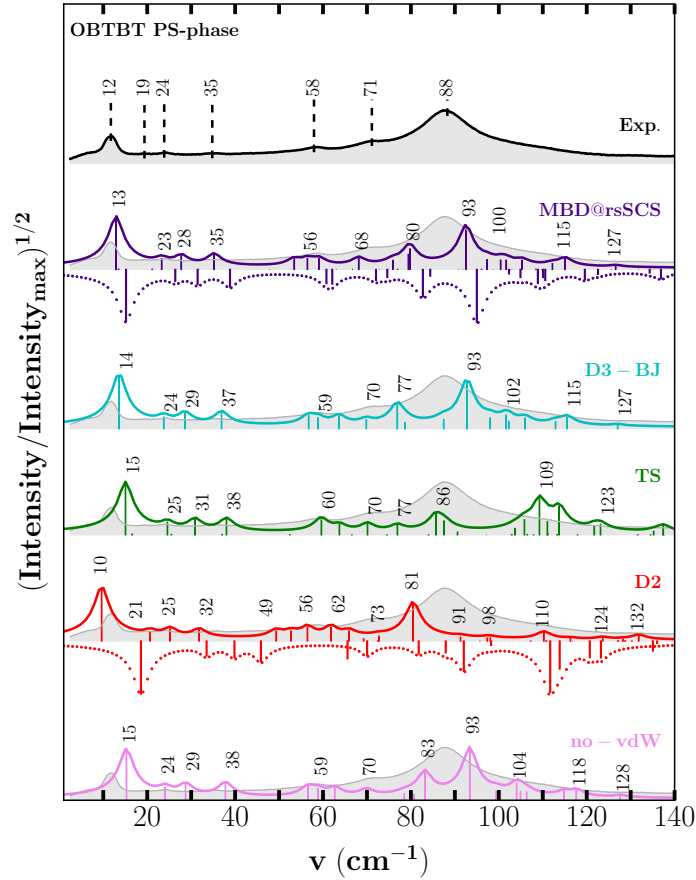
Figure 2: Experimental[32] and calculated Raman spectra of the PS-phase of the OBTBT molecule in the lattice phonon regime. To amplify smaller features, the square root of the intensities, normalized to the maximum intensity, is plotted instead of linear intensities. The Lorentzian functions around the calculated peak positions are drawn as a guide for the eye. Solid lines correspond to spectra calculated based on the experimentally determined unit cells. For the sake of comparison, the experimental data is replicated (shadowed in gray) below the calculated spectra. The dotted-downward spectra correspond to calculations performed at V_{calc} for the MBD@rsSCS and D2 cases.
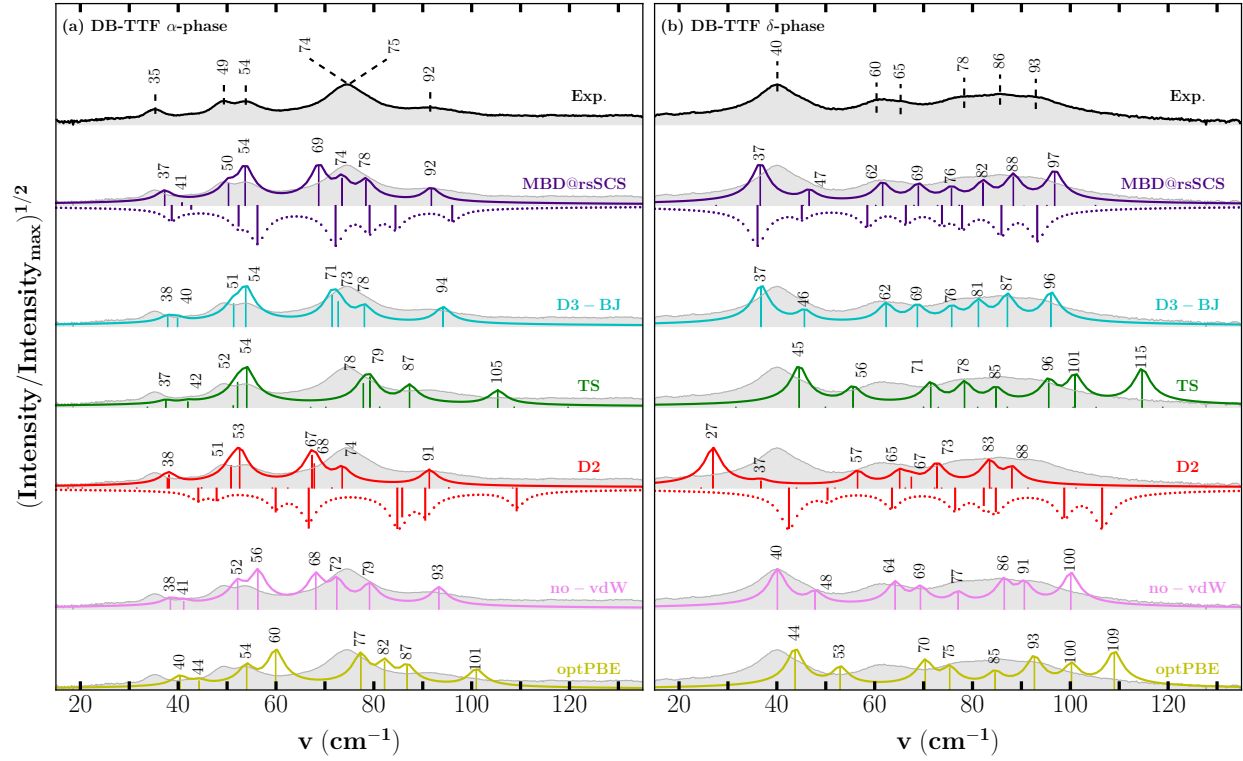
Figure 3: Experimental[48,49] and calculated Raman spectra of the (a) α-phase and (b) δ-phase of the DB-TTF molecule in the lattice phonon regime. Solid lines correspond to spectra calculated based on the experimentally determined unit cells. For the sake of comparison, the experimental data is replicated (shadowed in gray) below the calculated spectra. The dotted-downward spectra correspond to calculations performed at V_{calc} for the MBD@rsSCS and D2 cases.
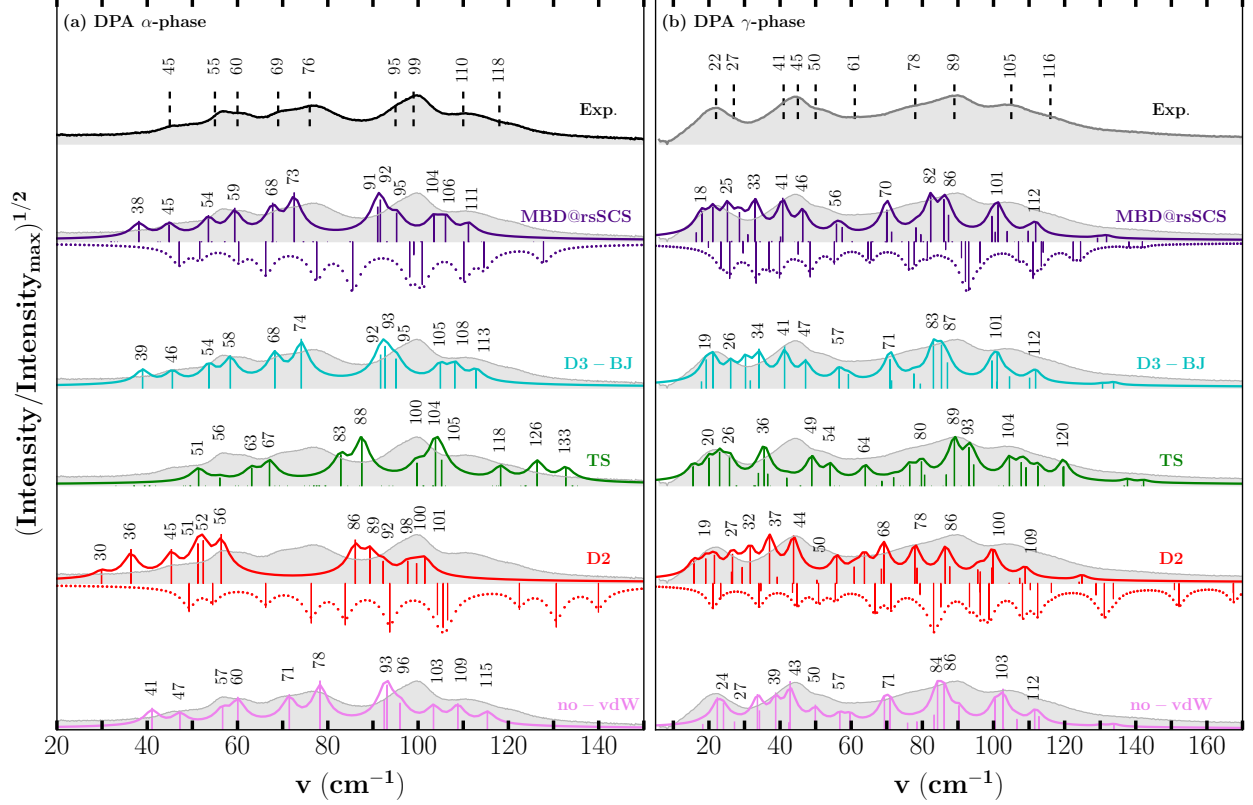
Figure 4: Experimental[50] and calculated Raman spectra of the (a) α-phase and (b) γ-phase of the DPA molecule in the lattice phonon regime. Solid lines correspond to spectra calculated based on the experimentally determined unit cells. For the sake of comparison, the experimental data is replicated (shadowed in gray) below the calculated spectra. The dotted-downward spectra correspond to calculations performed at V_{calc} for the MBD@rsSCS and D2 cases.

Below 80 cm^{-1}, the agreement between the MBD@rsSCS simulations and experiments is typically $\ll$ 4 cm^{-1}. In some cases, the positions of the high energy MBD@rsSCS Raman active modes ($>$ 80 cm^{-1}) are shifted by 5-7 cm^{-1} (e.g. the MBD@rsSCS calculated peak at 93 cm^{-1} for OBTBT, Fig. 2). In the particular case of the γ-phase of DPA (Fig. 4b) the richness of the spectra prevent an unambiguous peak assignment. Nonetheless, the broad distribution of bands in the experimental spectrum is consistent with the MBD@rsSCS calculated Raman active modes.

The excellent performance of the MBD@rsSCS approach to describe the Raman spectra of the studied systems is also observed for the D3-BJ method (blue curves Figs. 2-4). In all

cases the D3-BJ vdW-method reproduces the experimental spectra (deviation $\ll 4$ cm^{-1}) within the same accuracy as the MBD@rsSCS approach. Indeed, in most cases the positions of the D3-BJ calculated peak positions match the MBD@rsSCS values. These results are insofar relevant, as the D3-BJ approach is computationally significantly cheaper than the MBD@rsSCS method (see Sec. 3s in the Supporting Information). Moreover, the D3-BJ approach can serve as an accurate alternative for describing the lattice vibrations of systems for which the MBD@rsSCS method suffers from numerical instabilities.[54]

A much less accurate description of the lattice Raman spectra at V_{exp} is provided by the TS method (green curves Figs. 2-4). In this case, the Raman spectra of the considered polymorphs are described with an accuracy of 2 to 22 cm^{-1}. The largest error (22 cm^{-1}) is again observed for the high energy Raman active modes (> 80 cm^{-1}), in the same way as for the MBD@rsSCS and D3-BJ calculations. In certain cases, global shifts of the TS spectra toward higher frequencies relative to the experimental data are obtained (e.g. δ-DB-TTF and α-DPA, Figs. 3b, 4a). Notably, the effect is much more pronounced for the δ-phase of DB-TTF. This makes the use of scaling parameters, in analogy to the common practice for the simulation of intramolecular modes,[12,13] at best difficult, if not impossible. Moreover, a comparably good agreement with the experimental data is obtained for the PS-phase of OBTBT below 40 cm^{-1} (Fig. 2), and for the α-phase of DB-TTF below 60 cm^{-1} (Fig. 3a). The frequencies of higher-energy lattice Raman active modes in these cases, however, again have the tendency to be seriously overestimated (in certain cases up to 12 to 22 cm^{-1}). The seeming tendency for an overestimation of the positions of Raman-active modes by TS calculations is challenged by the observations for the γ-phase of DPA, where the calculated positions for most modes agree comparably well with the measured ones.

An accuracy of 2 to 15 cm^{-1} for the lattice Raman spectra of the studied polymorphs is obtained when applying the D2 vdW-correction method (red curves Figs. 2-4). The D2 calculated spectra are consistently shifted to lower wavenumbers relative to the other van der Waals correction schemes. For the PS-phase of OBTBT, the δ-phase of DB-TTF, and

the α-phase of DPA, this results in an underestimation of the peak positions compared to experiments, while the smaller shift for the α-phase of DB-TTF and the γ-phase of DPA results in a quite satisfactory agreement. Overall, contrary to the previously discussed vdW-methods, large errors are obtained for Raman active modes below ~ 50 cm^{-1}. This effect is particularly strong for the D2 spectra of the δ-phase of DB-TTF (Fig. 3b) and the α-phase of DPA (Fig. 4a). Such large errors for the lowest frequency modes are particularly problematic, as these modes are the ones that will become most strongly thermally occupied making them relevant for both, heat and charge transport.

Although the focus of the present paper is on the performance of a posteriori van der Waals correction schemes, for the sake of comparison, we also tested the performance of a non-local functional to describe the lattice vibrations of organic molecular crystals. Figure 3 shows the Raman spectra for the polymorphs of DB-TTF as predicted by the non-local functional proposed by Dion et al. and optimized for PBE (optPBE).[5,36] For none of the polyphorms the optPBE-vdW functional provides a description of the Raman spectra that would be comparable to the MBD@rsSCS or D3-BJ results. In fact, in both cases the agreement with respect to experiments is similar to that obtained in the case of TS, with a tendency to overestimate the positions of the Raman peaks.

An interesting observation is that DFT calculations which do not include vdW interactions (in the present case using the PBE functional), give Raman spectra as accurate as those obtained with the MBD@rsSCS and D3-BJ approaches, provided that the experimental volume is used. This is clearly shown by Raman spectra reported as "no-vdW" in Figs. 3-4 (pink curves), and Tables 6s-10s in the Supporting Information.

The comparison to experimental spectra provides the ultimate benchmark for the methodologies employed. However, the assignment between calculated and measured peaks can be ambiguous. Moreover, a peak in the experiment might arise from the superposition of Raman scattering processes at different phonon modes. Therefore, a more direct comparison between the performance of the different vdW approaches is instructive. The particular ad-

vantage here is that an unambiguous association of equivalent modes is straightforward on the basis of displacement patterns. Equivalent modes obtained with different vdW methods, and hence their frequencies, can be identified in a rigorous mathematical way as the ones with the largest dot product between their eigenvectors (equal to unity in the case of perfect agreement). Histograms of dot products, using the MBD@rsSCS method as a reference, are shown in Figs. 5a-e. Tables listing the equivalent vibrations and corresponding dot products are provided in the Supporting Information (Tables 6s-10s). Moreover, as separate files, animated comparisons of the first seven lattice vibrations of all systems and methods are supplied with the Supporting Information.

A key observation is that the MBD@rsSCS and D3-BJ displacement patterns for all considered systems are in very good agreement, with most of the dot products among their eigenvectors lying between 0.9 and 1.0 (see blue data in Figs. 5a-e). On the contrary, the agreement of the TS and D2 eigenvectors with those of MBD@rsSCS is poorer, with a much wider spread of dot products and with many values below 0.8 (see green and red data in Figs. 5a-e). This suggests that displacement patterns obtained using the TS and D2 schemes might be even qualitatively misleading when trying to understand the nature of the vibrations relevant for charge and heat transport.

A comparison of the frequencies obtained with the different vdW-methods is shown in Figs. 5f-j. These plots (together with the data in Tables 6s-10s in the Supporting Information) show that equivalent modes essentially keep their relative positions in the spectra. The MBD@rsSCS frequencies have the tendency to be overestimated by the TS method (green circles), and underestimated by the D2 scheme (red squares). This indicates that compared to MBD@rsSCS calculations the TS method yields a more pronounced increase of intermolecular forces with displacement, while the increase is smaller in the D2 case. The D3-BJ method, on the contrary, predicts frequencies in perfect agreement with the MBD@rsSCS data, consistent with the equivalence of their eigenvectors (see blue triangles in Fig. 5). A similar behavior is found when employing pure PBE, in the absence of any long-range vdW-

14

correction (magenta stars in Fig. 5). Frequencies and displacement patterns are in very good agreement with those obtained with MBD@rsSCS, with most of the dot product lying between 0.9 and 1.0 (see pink data in Fig. 5). A graphical comparison of the displacement patterns show that indeed the nature of the lattice vibrations is the same for MBD@rsSCS and PBE (see animations supplied in the Supporting information). Whether in our calculations this is a consequence of a fortuitous cancellation of errors, or whether it means that vibrations in the lattice-phonon region are hardly affected by vdW attractions and rather depend on inter-molecular repulsions cannot be conclusively answered by the available data. A good performance of PBE has recently also been reported for the band-dispersion of the lattice phonon modes of naphthalene by Brown-Altvater et al..[31] Conversely, for the two polymorphs of crystalline aspirin, Reilly and Tkatchenko[30] have shown that the inclusion of vdW corrections in the MBD@rsSCS flavor is necessary to accurately describe the lattice vibrations. This is suggested to be necessary to account for the coupling between lattice vibrations and collective electronic fluctuations. This coupling has shown to be responsible of the softening of the lattice vibrations of the most stable polymorph of aspirin.[30,55] This implies that pure PBE might not be a generally reliable method for simulating lattice vibrations of molecular crystals.
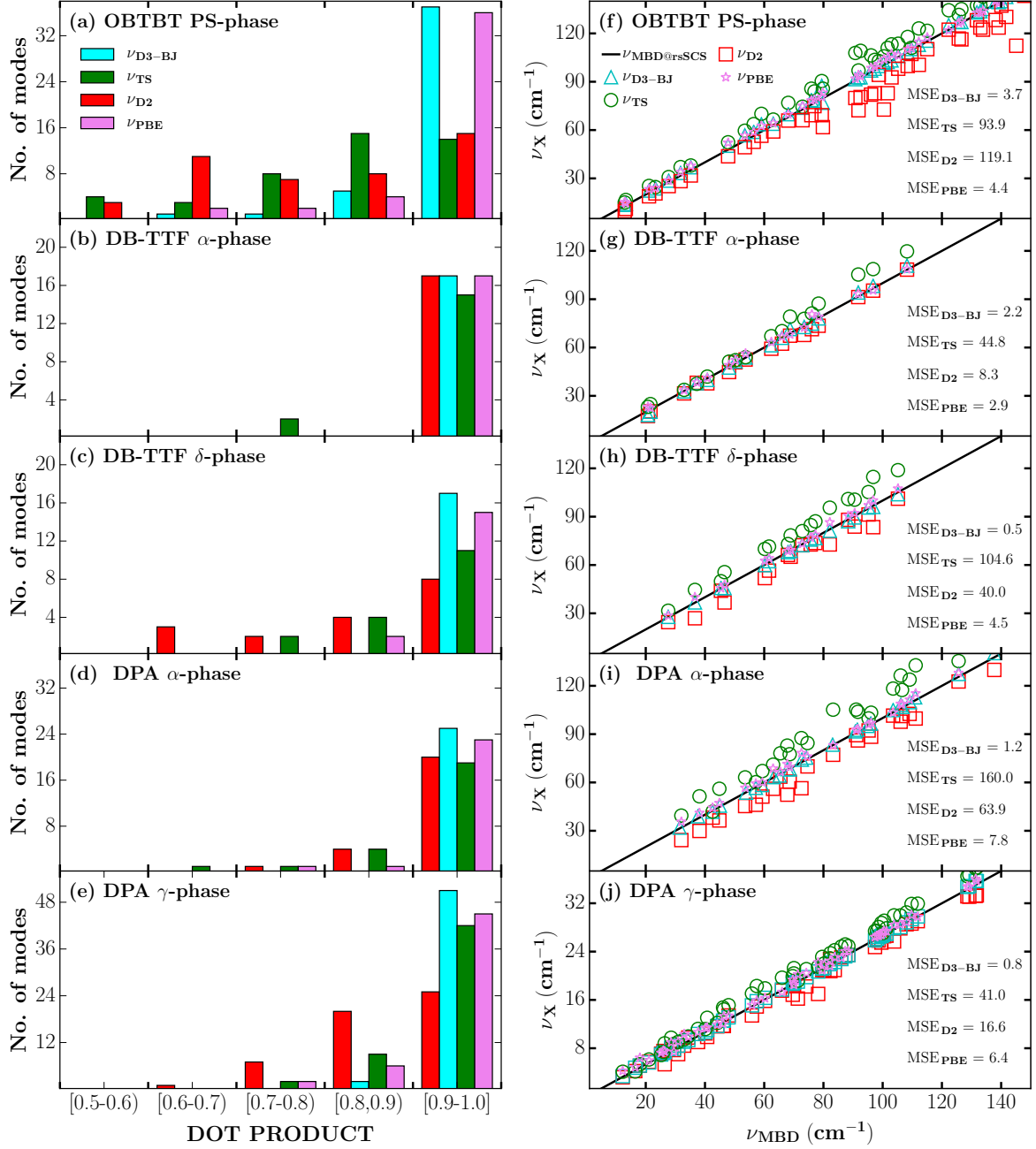
Figure 5: (a)-(e) Distribution of dot products between the lattice eigenvectors obtained with MBD@rsSCS and those calculated with D3-BJ, TS, D2 and no-vdW. (f)-(j) TS (ν_{TS}), D2 (ν_{D2}), D3-BJ ($\nu_{\text{D3-BJ}}$) and no-vdW (ν_{PBE}) lattice frequencies as a function of those calculated with MBD@rsSCS ($\nu_{\text{MBD@rsSCS}}$). Mean-square-errors are reported inside the graphs. Tables 6s-10s, in the Supporting Information, list the data used for these plots.

16

3.2 Lattice parameters optimization

A definite shortcoming of vdW-free DFT calculations is that they will typically fail in calculating the equilibrium lattice parameters of molecular crystals held together by van der Waals forces. I.e, such simulations will have to rely on experimentally determined unit cells.

Considering that a reliable description of the unit-cell parameters is crucial to predict lattice phonon modes of organic molecular crystals in the absence of structural data, we have assessed the accuracy of the different vdW-corrections employed for that task. Here, we restrict ourselves to the situation encountered when approaching zero Kelvin. It should be remarked that zero-point energies were not considered for the relaxation of the volumes. This would require phonon-calculations beyond the Γ-point in the quasi-harmonic approximation (i.e. for different volumes), which are beyond the scope of this work, and very likely beyond the capacities of present computational resources especially for the larger unit cells. For simple systems like carbon dioxide, ice, acetic acid and imadazole it has recently been shown that volume relaxations including zero-point energies could yield volumes 2-3 % higher than those predicted from lattice energy relaxations.[56–58] We expect this effect to be much smaller for the comparably heavy molecules studied here, but those observations still suggest that the calculated unit-cell volumes reported in the following represent lower limits to the actual situation at low temperatures. A further aspect to be considered is that the experiments to which we compare our calculations have been performed typically at room temperature. If we were able to include the corresponding thermal expansion in the simulations, an additionally increase of the calculated volumes would occur. Consistent with these considerations, in most cases the calculations predicted smaller volumes compared to the experimental values, as shown in Table 1. The only outliers are the MBD@rsSCS and TS relaxed volumes of the δ-phase of DB-TTF, which slightly overestimate the experimental values. For this system, however, experiments were performed at relatively low temperatures (93.1 K).

In order to assess the accuracy of the calculated positions of the individual atoms constituting the molecules, we compared the experimental and calculated relaxed structures,

17

using the distance comparison method (see Methodology Section). This yielded root-mean-square-deviations (RMSD) between atomic positions ranging from 0.07 Å to 0.36 Å (see Table 1), which are well below 1.0 Å, the normally adopted threshold to determine whether a structure is correctly calculated.[59,60]

Comparing the different vdW approaches, the volumes obtained in the MBD@rsSCS and TS simulations are very close to each other (typically within $\sim$ 1-2%) and rather close to the experiments. The D2 approach systematically predicts the most tightly packed systems with unit cell volumes up to 10 % below those obtained experimentally. The D3-BJ approach in all cases underestimates the experimental volumes by 1.4-4.7 %. In certain cases it predicts values in good agreement with TS and MBD@rsSCS data (PS-OBTBT and α-DPA), while there are systems for which it yields unit cells as tightly packed as those obtained in the D2 calculations (α-DB-TTF).

Table 1: Comparison between calculated (V_{calc}) and experimental (V_{exp}) volumes for the considered systems. Volumes were obtained from lattice energy relaxations. In parenthesis relative differences between V_{exp} and V_{calc} are provided in percent. In the case of experimental data the numbers in parenthesis are the standard uncertainties in the final digits (when available). The RMSD values were calculated following the distance comparison method, as described in the Methodology Section. The lattice parameters are reported in Table 11s in the Supporting Information.

		T (K)	volume (Å^3)	RMSD (Å)
PS OBTBT triclinic	EXP[52,53]	123	1324.76(13)	–
	MBD@rsSCS	–	1296.12(-2.2)	0.11
	D3-BJ	–	1299.59(-1.9)	0.08
	TS	–	1286.34(-2.9)	0.15
	D2	–	1208.95(-8.7)	0.23
α DB-TTF monoclinic	EXP[48]	300	634.57	–
	MBD@rsSCS	–	625.77(-1.4)	0.11
	D3-BJ	–	605.25(-4.6)	0.13
	TS	–	619.78(-2.3)	0.10
	D2	–	598.52(-5.7)	0.14
δ DB-TTF triclinic	EXP[49]	93.1	628.42(5)	–
	MBD@rsSCS	–	638.90(1.7)	0.10
	D3-BJ	–	616.78(-1.9)	0.07
	TS	–	631.07(0.4)	0.07
	D2	–	607.97(-3.3)	0.10
α DPA monoclinic	EXP[51]	293	1774.45	–
	MBD@rsSCS	–	1705.01(-3.9)	0.11
	D3-BJ	–	1692.59(-4.6)	0.12
	TS	–	1697.07(-4.4)	0.11
	D2	–	1614.94(-9.0)	0.22
γ DPA monoclinic	EXP[50]	300	1818.83(7)	–
	MBD@rsSCS	–	1732.85(-4.7)	0.12
	D3-BJ	–	1715.21(-5.7)	0.19
	TS	–	1700.08(-6.5)	0.21
	D2	–	1635.26(-10.1)	0.36

3.3 Calculated Raman spectra at relaxed volumes

In order to quantify the impact of the volume relaxation on the vibrational properties, we calculated the lattice Raman spectra at the relaxed volumes for the MBD@rsSCS and D2 vdW-approaches, which typically provide the smallest and the largest changes in volume relative to the experimental data (see Table 1).

For all systems in which the unit-cell volume is smaller in the simulations this results in a shift of the peaks to higher wavenumbers, see downward-dotted spectra in Figs. 2-4. In the particular case of the δ-phase of DB-TTF, the MBD@rsSCS Raman spectra shifts in the opposite direction, as expected considering the overestimated optimized volume. Nevertheless, even here the agreement between measured and calculated spectra is best when employing the experimental volume (see shaded and downward-dotted purple curves in Figs. 2-4). This makes sense considering that both the x-ray diffraction experiments and the Raman spectroscopy were performed at temperatures much higher than zero Kelvin. Overall, the impact of the volume on the MBD@rsSCS lattice vibrations is comparably small, with average changes $< 4 \text{ cm}^{-1}$, see Figs. 6a-e and Tables 12s-16s in the Supporting Information. This is consistent with the rather small change in volume.

In the D2 case, the impact of relaxing the unit-cell is more extreme, with Raman peaks shifting by up to 25 cm^{-1}, in agreement with the large volume changes predicted by this method. In relative numbers, for OBTBT this means that some frequencies change by $\sim 50\%$, while the first Raman lattice vibration even essentially doubles (see shaded and downward-dotted red curves in Fig 2). As in the D2 simulations using the experimental unit cell the positions of the Raman active modes had been underestimated, the large shift to higher wavenumbers at the relaxed volumes in some instances improves the agreement with experiments. At least, it does not massively deteriorate the situation, albeit now the D2 calculations typically over- rather than underestimate the experimentally determined frequencies.

For the D2 case, the entire set of lattice vibrations change on average $\sim 19 \text{ cm}^{-1}$, which is much larger than for the MBD@rsSCS case ($< 4 \text{ cm}^{-1}$), see Tables 12s-16s. As a consequence, the average mean square deviation between the frequencies calculated at V_calc and at V_exp is by an oder of magnitude larger than for the MBD@rsSCS case [$\sim 337 \text{ (cm}^{-1})^2$ vs. ~ 41 cm^{-12}], see Figs. 6a-e.

Besides analyzing the impact of the volume relaxation on the frequencies, it is interesting

to asses the change of the eigenvectors. Figures 6f-j show histograms of the dot products between the eigenvectors calculated at V_{calc} and V_{exp}. In all cases the MBD@rsSCS eigenvectors calculated at the two different volumes change much less than those obtained with the D2 method. Most of the dot products obtained for MBD@rsSCS lie between 0.9 and 1.0, while the D2 method shows a broader distribution with values between 0.5 and 1.0. Not unexpectedly, the broadest distribution of dot products for D2 is obtained for the γ-phase of DPA, for which the D2 method predicts the largest change in volume. Notably, for OBTBT also a very broad spread of the dot products is observed, in this case even for the MBD@rsSCS method. This can be attributed to the comparably complex structure of OBTBT, with a rigid core and flexible aliphatic side-chains, that may result more sensitive to the change in volume.
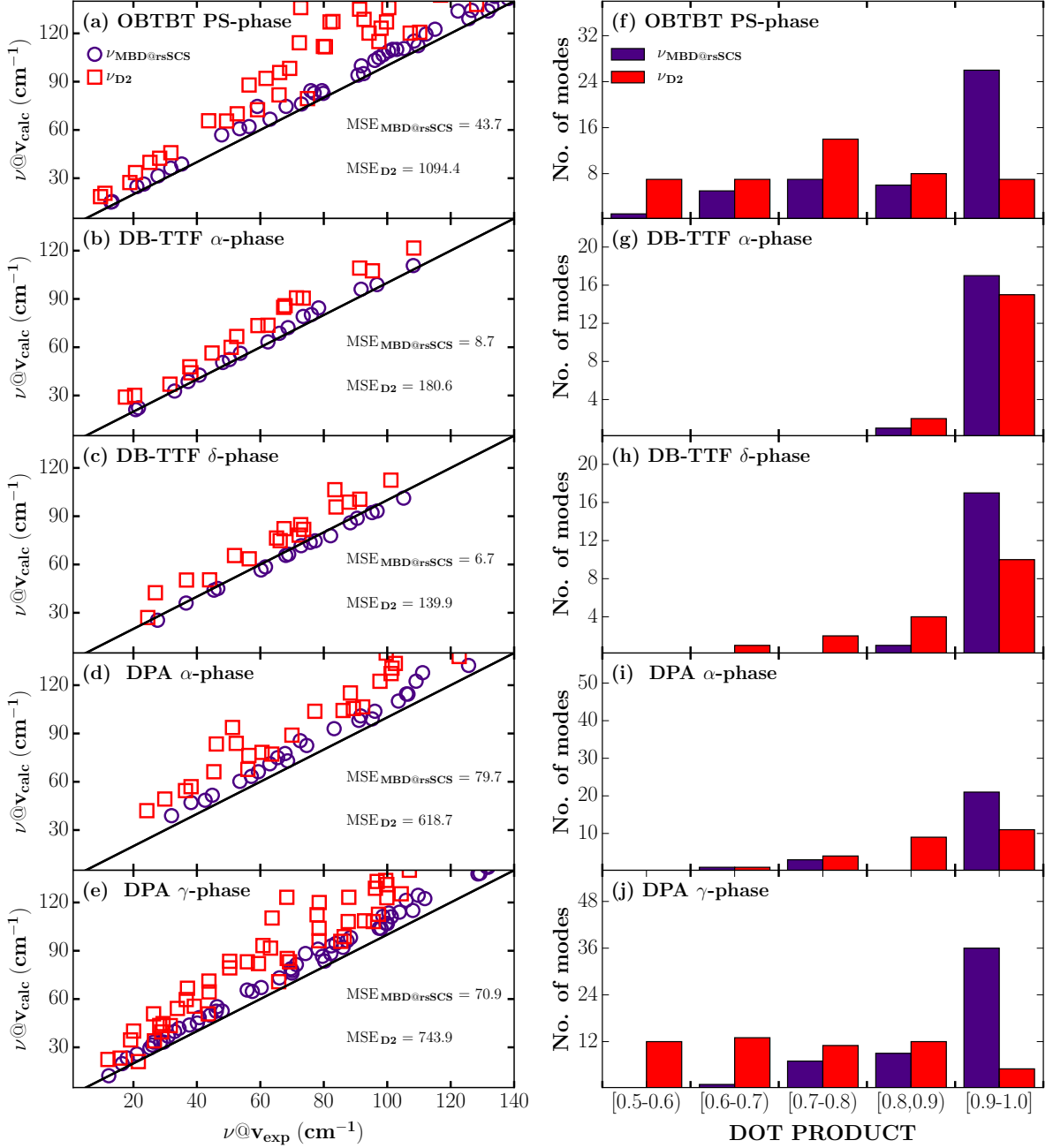
Figure 6: (a)-(e) Lattice frequencies calculated at V_{calc} as a function of those obtained at V_{exp} for MBD@rsSCS and D2. The black lines denote the virtual case in which frequencies do not depend on the volume (i.e. V_{exp} against V_{exp}). Mean-square-errors are reported inside the graphs. (f)-(j) Distribution of dot products between the lattice eigenvectors obtained at V_{exp} and V_{calc} when using MBD@rsSCS and D2. Tables 12s-16s, in the Supporting Information, list the data used for these plots.

4   Summary and Conclusions

We assessed the performance of four different a posterior vdW methods to account for long-range vdW interactions in local DFT. The performance was evaluated by comparing calculated and measured lattice Raman spectra in the low-wavenumber region (< 150 cm^{-1}) for several polymorphs of different molecular crystals. The spectra in that range are particularly suited for that purpose, as they are typically dominated by intermolecular vibrations, for which a significant dependence on van der Waals interactions can be expected. Amongst the tested methodologies, the most reliable and systematic description of the vibrational properties was found for the MBD@rsSCS and D3-BJ approaches. These methods not only provide the best overall agreement with the experimental spectra, but comparing the computational results also yield fully consistent frequencies and eigenvectors. From a practical point of view it is interesting to mentioned that the excellent performance in the D3-BJ scheme is achieved at significantly reduced computational costs. The accuracy of the TS and D2 vdW-correction schemes is typically lower and varies considerably depending on the system and the wavenumber range. The lack of a general trend in these cases also prevents the determination of ad hoc scaling parameters for the frequencies, as usually employed for high-energy molecular vibrations.

For the sake of comparison, we also tested the non-local functional vdW-DF-optPBE for two of the studied polymorphs, where we observed an accuracy of the same order as for the TS and D2 approaches (i.e. worse than in the MBD@rsSCS and D3-BJ calculations).

Interestingly, also in PBE simulations disregarding a posteriori van der Waals corrections, an excellent agreement between theory and experiment is obtained for the systems considered here, as long as experimentally determined unit-cell geometries are employed.

As far as the prediction of the structural parameters of the different systems is concerned, all employed a posteriori van der Waals corrections provided a satisfactory agreement. The best fit between simulations (disregarding thermal expansion) and experiments (at finite temperatures) was obtained for the MBD@rsSCS and TS approaches, closely followed by

the D3-BJ. Only for the D2 approach, changes of the equilibrium volume amounted to up to 10%. Employing the relaxed rather than the experimental volumes, for the tested methods (MBD@rsSCS and D2) we typically observed a shift of the spectra to higher wavenumbers. This effect was particularly pronounce in the D2 case with several frequencies increasing by $> 50\%$. This, however, did not fundamentally improve the performance of the D2 method compared to the experimental Raman spectra.

Overall, this work establishes a frame of reference for the computational study of vibrational properties of organic molecular crystals in the lattice phonon range. This is distinct relevance, as these vibrations crucially determine, for example, charge- and heat-transport processes. Therefore, we expect that the accurate vibrational properties obtained when employing the MBD@rsSCS and D3-BJ approaches will in the future help to gain unprecedented insights into the relationship between the structures of molecular crystals and a number of their relevant physical properties.

Acknowledgement

Supporting Information Available

Detailed information about k-grid points sampling and PAW potentials used in the simulations, as well as complementary results are provided in the Supporting information (PDF). Animations comparing the first seven lattice vibrations reported in Tables 6s-10s (ZIP). This material is available free of charge via the Internet at `http://pubs.acs.org/`.